

1 **Temporal analysis (1940–2010) of rainfall aggressiveness in the**

2 **Iberian Peninsula basins**

3 **L. García-Barrón^{1*}, J.M. Camarillo², J. Morales³, A. Sousa³**

4

5 ¹*Departamento de Física Aplicada II, Universidad de Sevilla, 41012 Sevilla, Spain*

6 ²*Departamento de Geografía Física, Universidad de Sevilla, 41004 Sevilla, Spain*

7 ³*Departamento de Biología Vegetal y Ecología, Universidad de Sevilla, 41012 Sevilla, Spain*

8 **ABSTRACT**

9 Rainfall aggressiveness causes environmental impacts and it is related to several natural
10 hazards. Therefore, this parameter has been chosen as an environmental indicator. The
11 present study is based on the monthly estimated rainfall using the Precipitation Runoff
12 Integrated Model (SIMPA) for each Spanish hydrographic basin from 1940 to 2010. The
13 main aim is to analyse temporal irregularity of rainfall aggressiveness in large geographic
14 areas and to extract spatio-temporal patterns. For each year the rainfall aggressiveness was
15 calculated using the Modified Fournier Index (I_{FM}) and Oliver's Index of Precipitation
16 Concentration (I_{PC}). The temporal variability of the annual series of these indices was
17 analysed for each zone delimited. The results obtained made it possible to characterize the
18 rainfall aggressiveness in the Iberian Peninsula and to determine its evolution over the past
19 decades. They also reveal that the general pattern of the rainfall aggressiveness is
20 determined by the dual effect of latitude (north–south) and longitude (east–west) as a result
21 of the different maritime influences of the Atlantic and the Mediterranean watersheds.

* Corresponding author: Tel.: + 34 954 55 67 82.

E-mail addresses: leoncio@us.es (L. García-Barrón).

22 Finally a new variable is proposed, the Annual Aggressiveness Risk R_A , which summarizes
23 the information provided by I_{FM} and I_{PC} .

24 **Keywords:** rainfall aggressiveness, concentration index, irregularity, basin, Spain

25

26 **1. Introduction**

27 Changes in rainfall intensity cause environmental impacts and are related to various natural
28 hazards (Estrela et al, 2012;. Machado et al., 2001). Therefore, knowledge of the spatial and
29 temporal variability of precipitation is relevant to characterize the regime of the hydrological
30 basins, its exposure to risks and, if applicable, the adoption of prevention and mitigation
31 measures (Krysanova et al., 2010; Middelkoop et al., 2001). In this paper we focus on
32 estimating the aggressiveness of rainfall as an indicator of potential environmental impact. It
33 is especially important to know the temporal evolution of the rainfall aggressiveness in areas
34 like the Iberian Peninsula, which is characterized by irregular inter-annual and intra-annual
35 precipitation (García-Barrón et al 2011, 2013).

36 The Iberian Peninsula is located in the climatic transition zone between the mid-latitudes
37 and the subtropical climates, and it presents complex orographic features that influence the
38 generation of precipitation. Furthermore, its peculiar geographical location between the
39 Mediterranean Sea and the Atlantic Ocean determines a wide range of Mediterranean
40 climates (De Castro et al., 2005) whose different rainfall characteristics reflect a wide range
41 of landscape and environmental varieties. The peninsula's hydrological basins, except the
42 Cantabrian one, show the characteristics associated with the Mediterranean climate:
43 variability of rainfall, wet years mixed with recurrent droughts, high concentrations of
44 rainfall over a few days and low rainfall during the summer (Lionello et al., 2006; Martín-
45 Vide and Olcina, 2001).

46 We believe that the river basin is an appropriate spatial scale for assessing the natural
47 hazards associated with rainfall, being the natural hydro-climatic area (González-Hidalgo et
48 al., 2010). Several authors have also considered the river basin as the territorial unit for the
49 analysis of precipitation and its impact (Angulo-Martínez et al., 2009; Barriendos and
50 Rodrigo, 2006; Caramelo and Manso-Orgaz, 2007; González-Hidalgo et al., 2010; Kilsby et

51 al., 2007; López-Moreno et al., 2013; Morán-Tejeda et al., 2012; Valencia et al., 2012).
52 Therefore, understanding the evolution of aggressivity in each basin during the last decades,
53 is crucial in order to undertaking water resource management and planning, including the
54 water supply to populations, the organization of irrigation, the water infrastructure design,
55 the flood and drought management, etc. To do this, it is necessary to develop new
56 procedures that provide information about the behaviour of the hydrology of each studied
57 zone over long periods.

58 Trends and the interannual and intra-annual variability at different time scales have been
59 analysed with different approaches (Acero et al., 2011; Costa et al., 2012; De Luis et al.,
60 2010a; Del Río et al., 2011; García et al., 2007; García-Barrón et al., 2011, 2013; Lorenzo-
61 Lacruz et al., 2012; Martín-Vide, 2004; Sousa et al., 2010). The impact of rain on
62 agriculture and forestry (Nippert et al., 2006; Pérez-Camacho et al., 2012; Sardans and
63 Peñuelas, 2013), on erosion and desertification (Briggs et al., 1992; De Vente et al., 2008;
64 Diodato et al., 2011; Vicente-Serrano, 2006) and on hydrology (Do Ó, 2010; Embid and
65 Gurrea, 2004; Sousa et al., 2013) have also been widely studied from different perspectives.

66 From this point of view, it is important to analyse environmental indicators and to identify
67 patterns that make it possible to infer consequences for large territorial areas. In this paper,
68 the Spanish territory of the Iberian Peninsula has been divided into zones, largely coincident
69 with the Spanish hydrographic basin; each one is represented by its total annual rainfall
70 values and its intra-annual distribution. We selected rainfall aggressiveness as an
71 environmental indicator parameter that will broaden the knowledge about the spatial
72 variability of precipitation patterns in the zones.

73 Knowledge of rainfall aggressiveness is linked to several environmental study fields. Its
74 effects are related to torrentiality, erosivity, landslides, floods, silting, etc. (Diodato et al.,
75 2011; Gregori et al., 2006; Sousa et al., 2013). As an environmental indicator, it is based on

76 the calculation of the Modified Fournier Index (I_{FM} from now on) (Arnoldus, 1980;
77 Fournier, 1960), and it is complemented by the Precipitation Concentration Index (I_{PC}
78 hereafter) (Oliver, 1980).

79 Both indices are based on monthly rainfall records. Some environmental impacts depend on
80 the rainfall intensity of each event but, except for the modern automatic weather stations,
81 traditional stations do not have high frequency rainfall records (in minutes). Moreover,
82 torrential rain events in the Mediterranean area are often highly concentrated.

83 For example, for the direct calculation of rainfall erosivity at a regional scale (Angulo-
84 Martínez et al., 2009) it is convenient to use a set of closely spaced (<15 km) weather
85 stations, each of which holds high frequency records for at least twenty years. In Spain, the
86 rain gauge network is recent, scarce and unevenly distributed; therefore, it is not possible to
87 directly analyse the evolution of impacts using a network of high frequency local records
88 across large regions over the course of a long period of time. Thus, to obtain information
89 about the potential risks of rainfall in the area that have sufficient spatial and temporal
90 validity, it is necessary to use alternative methods based on monthly data, as proposed in this
91 work.

92 The usefulness and value of this new methodological approach, based on monthly rainfall
93 data, is that it allows reconstructing the evolution of the rainfall aggressiveness in the large
94 river basins of the Iberian Peninsula during the period 1940-2010. Subsequently, this
95 approach can be used as a basis for linking the rainfall aggressiveness with hydrological
96 processes that can have a great impact, such as the evolution of soil erosion, the silting of
97 reservoirs, etc. The high rainfall variability entails a significant irregularity of the
98 environmental effects associated with precipitation. Different studies of rainfall
99 aggressiveness have been made from rainfall records. Gregori et al. (2006) highlighted the
100 enormous versatility of the Modified Fournier Index (I_{FM}) to describe the characteristics of

101 the rainfall regime and its relationship to some instability phenomena (quick flows,
102 erosivity, shallow landslides etc.). Michiels et al. (1992) used the I_{PC} to describe the
103 variability of rainfall in the Iberian Peninsula and considered that it was suitable to evaluate
104 erosivity. De Luis et al. (2010b) executed both the I_{FM} and the I_{PC} to study the possible
105 increase in erosivity in the Spanish Mediterranean area from a wide range of selected
106 weather stations. I_{PC} has also been employed with monthly data from scattered weather
107 stations across the Iberian Peninsula to analyse the temporal trend in rainfall and to describe
108 spatial patterns (De Luis et al., 2011). In general, these papers focus on the analysis of
109 annual or seasonal trends. In addition, there are many precedents for the use of these indices
110 of aggressiveness (the I_{FM} and the I_{PC}) and the analysis of their relationship with other
111 parameters in the Mediterranean area (Apaydin et al., 2006; Diodato and Belocchi, 2007)
112 and in different climatic areas and different continents (Da Silva, 2004; Diodato et al., 2013;
113 Elagib, 2011; Febles et al., 2009; Gabriels, 2006; Lee and Heo, 2011; Munka et al., 2007;
114 Rey et al., 2012; Sauerborn et al., 1999 Vrieling et al., 2010). However, we believe that the
115 analysis of the multi-annual irregularity of the indices proposed in this paper and applied to
116 large basins provides an innovative approach that could broaden the study perspective.
117 For all these reasons, we intended to determine the specific temporal behaviour of rainfall
118 aggressiveness in each zone and to establish the relationships between the different climatic
119 areas in order to extract general patterns, if possible. Thereby, the overall objective of the
120 study was to determine the evolution of rainfall aggressiveness during the period 1940–2010
121 in the defined Spanish zones. More specifically, by using the time series generated for both
122 the I_{FM} and the I_{PC} the intentions were:

- 123 - To characterize the temporal irregularity of aggressiveness in each zone delimited by the
- 124 comparative analysis of trends, interannual variability and disparity.

125 - To check whether the results reveal similarities and differences between the zones that
126 allow for the establishment of a spatial pattern for each watershed (Mediterranean/Atlantic)
127 or for the whole Iberian Peninsula.

128 The indicators of the rainfall intensity that we developed in this study allow a comparative
129 analysis of the evolution of the rainfall aggressiveness in different basins for an extended
130 period (1940-2010). As a result of this comparative analysis it is possible that a general
131 pattern of evolution in the Iberian Peninsula, which may be supplemented by variations
132 according to the geographic location, appears. The knowledge of these patterns of variation
133 could have interesting implications for water planning (management of water resources,
134 conservation of rivers, flow regulation, assessment of river ecosystems, ...) and, generally,
135 for the development of environmental policies, besides serving as a basis for further studies
136 of climate change scenarios.

137 **2. Study area and data**

138 The study area is the Spanish territory of the Iberian Peninsula, which is divided into large
139 basins which are largely coincident with the boundaries of the Spanish hydrographic basins.
140 We chose to aggregate small adjoining basins. The Water Information Service (Sistemas de
141 Información del Agua, SIA in Spanish) of the Ministry of Agriculture, Food and
142 Environment of Spain is responsible for the quality of water resources and environmental
143 status management, and it is also in charge of the water risk prevention in the Spanish
144 hydrographic basin.

145 In collaboration with some university departments, this service has developed the Sistema
146 Integrado de Modelización Precipitación-Aportación (Precipitation Runoff Integrated
147 Model) known as SIMPA (Estrela and Quintas, 1996). For climate information, SIMPA
148 estimates the rainfall for each Spanish hydrographic basin, month by month throughout the
149 simulation period, from data recorded by selected rain gauges of the official networks,

150 which include the Spanish Meteorological Agency (Agencia Española de Meteorología,
151 AEMET), the Spanish Hydrographic Service, etc. (Estrela et al., 1999; Ministerio de
152 Agricultura, Alimentación y Medio Ambiente, 2013). SIMPA takes monthly precipitation
153 from 1 km grid maps created by the Spanish Ministry of Environment by means of an
154 interpolation procedure (the inverse to the square distance) with data from the more than
155 5000 weather stations of the Spanish network (Belmar et al., 2011). For this interpolation,
156 double regression and “white noise” procedures were used to complete incomplete series
157 without altering the natural variance of data, as well as specific procedures for the highest
158 elevation areas (Estrela et al., 1999). The lack of rain gauges in the highest regions produces
159 significant underestimations of the rainfall of many headwaters. To overcome this, SIMPA
160 generated a rainfall time series based on specific regional algorithms analysing the factors
161 that influence the process (precipitation, altitude, orientation, slope, etc.). The location of the
162 stations used is available at Estrela et al. (1999) o MIMAM (2000). The SIMPA model has
163 been frequently used to study hydrological processes in Spanish basins (Belmar et al., 2011;
164 Bejarano et al., 2010; Chavez-Jiménez et al., 2013; Sánchez et al., 2011). The basic monthly
165 datasets used in this study are the official SIA series, which are considered to be
166 homogeneous and without gaps.

167 The capacity of synthesis of the SIMPA model, from the records of 5000 meteorological
168 stations, has the advantage of being suitable for analysing reliably the development of
169 estimated rainfall in large natural areas and over long periods. The development of a single
170 dataset of rainfall representative of each case study area allows results to be obtained that
171 enable direct comparisons to be made between all of the areas, including their evolution.
172 This study covered the period from September 1940 to August 2010, and it considered the
173 hydrological year. For this, ten zones were distinguished for the Spanish mainland (Fig. 1).

174 The zones are groups of basins, and the rainfall assigned to each zone was calculated from
175 the monthly rainfall of each, weighted by their respective surfaces.

176 *Fig.1 around here*

177 With regard to the zones shown in Fig. 1, the Cantabrian zone (25,343 km²) is formed by the
178 basins of the northern slopes of the Cantabrian mountains that flow into the sea of the same
179 name. The Atlantic watershed is composed of the Galicia zone, the Plateau [Meseta in
180 Spanish] zones (the basins of the Douro [Duero in Spanish], Tagus [Tajo in Spanish],
181 Guadiana) and the Guadalquivir zone. The Galicia zone (34,056 km²) is formed by the
182 grouping of the Miño-Sil river basin (52%) with other minor basins of this region. The
183 Spanish basins of the rivers Douro (78,859 km²), Tagus (55,764 km²) and Guadiana (55,468
184 km²) form their own zone. The Guadalquivir zone (57,700 km²) groups the Guadalquivir
185 river basin (87%) and that of other minor Andalusian rivers draining to the Atlantic.

186 The Mediterranean watershed is formed by the Jucar and Ebro Rivers, the Southeastern zone
187 and the Catalanian zone. The Southeastern zone [Sureste in Spanish, SE] (40,128 km²) is
188 formed by the Andalusian Mediterranean (50%) and the Segura basins (50%). The Jucar
189 (45,118 km²) and Ebro (85,900 km²) river zones are constituted solely by their respective
190 basins. The Catalanian zone (18,047 km²) is formed by the basins of small rivers within this
191 region. The percentages in parentheses indicate the proportion of the area of the respective
192 river basin district relative to the total area of the zone that it is included in.

193 **3. Methodology**

194 The present study is based on the analysis of the rainfall aggressiveness in the ten
195 hydrological zones that appear in Fig.1. The annual precipitation series from 1940 to 2010
196 were prepared for these zones (Fig.1). Calculating the potential aggressiveness of the
197 precipitation was carried out using the Modified Fournier Index (I_{FM}):

$$198 \quad I_{FM} = (\sum p_m^2)/P \quad (1)$$

199 where p_m is the monthly rainfall for each month ($m = 1, 2, \dots, 12$), and P is the corresponding
200 total annual precipitation. However, it has been observed (García-Barrón et al., 2010) that
201 high values of the I_{FM} index correspond to high total annual precipitation, so we believe that
202 the intra-annual distribution is undervalued. Therefore, we also used jointly the Precipitation
203 Concentration Index (I_{PC}).

$$204 \quad I_{PC} = 100 (\sum p_m^2) / P^2 \quad (2)$$

205 This index provides a dimensionless value for each year, which depends on the intra-annual
206 distribution of rainfall, but it is independent of the size of the total value. If two different
207 years Year A and Year A' have the same intra-annual distribution, namely the precipitation
208 of the corresponding months are proportional $p_m = kp_m'$, where k is a constant, then the value
209 of the $I_{PC} = I_{PC}'$ index is the same for both. The significance of the I_{PC} index is that it reveals
210 that a high temporal concentration of rainfall can cause more severe impacts on the
211 environment.

212 In our opinion, the combined interpretation of both indices provides more complete
213 information on the rainfall aggressiveness since it allows the temporal irregularities of each
214 zone to be characterized and analysed to identify the contrast in behaviour between them.
215 Years that are considered to be at risk of aggressive rainfall are those where I_{FM} and I_{PC} are
216 high. Conversely, simultaneously low I_{FM} and I_{PC} values indicate years of low and scattered
217 annual rainfall, thereby reducing the potential aggressiveness of the rain.

218 The analysis of the annual series of potential aggressiveness I_{FM} and concentration I_{PC} aims
219 to identify temporal irregularity. The following were used to highlight the temporal
220 irregularity: the coefficient of variation for each complete series, the mobile variation
221 coefficient using periods of eleven years, the indices of general and specific disparity, and
222 the analysis of trend. These methods were applied successively to the two sets of indicators.

223 A similar methodology has been proposed by the authors in previous works (García-Barrón
 224 et al., 2011, 2013) for the study of direct datasets of rainfall, but the application of the
 225 analysis of the space-time irregularity of these indicators of aggressiveness is considered
 226 novel.

227 The mobile variation coefficient using periods of eleven years is defined as the ratio of the
 228 standard deviation of the partial subset formed by the reference year i and the previous ten to
 229 the corresponding mean

$$230 \quad V_{i(11)} = \sigma_{(i, i-10)} / \mu_{(i, i-10)} \quad (3)$$

231 Choosing an eleven year period, coinciding with the solar cycle, allows the smoothing of
 232 extreme annual values and highlights the sequence variability in the long-term time series
 233 (García-Barrón et al., 2011; Rodrigo and Trigo, 2007). Because of the complexity of the
 234 climate system, meteorological variables do not always show clear, unambiguous
 235 periodicities. Our choice of an eleven year period, corresponding to the solar cycle, is based
 236 on an objective criterion of energy-climate regulation (Dima et al., 2005).

237 The coefficient of variation of the entire series is referred to as V_N .

238 The general disparity index I_D is calculated as the square root of the sum of squares of
 239 consecutive deviations extended to all the calculated series, divided by the number of
 240 summands, and in turn divided by the mean value μ_R of the complete series. Thus, if r_i is a
 241 value calculated for the year i and r_{i+1} for the following year, then

$$242 \quad I_D = (\{ \Sigma[(r_{i+1} - r_i)^2] / N - 1 \}^{1/2}) / \mu_R \quad (4)$$

243 The specific disparity index for the year i , I_{di} , considers only the elements $\{r_{i-1}, r_i, r_{i+1}\}$ of
 244 the time series, μ_i being the average of the three consecutive elements centered on i .

$$245 \quad I_{di} = (\{ [(r_i - r_{i-1})^2 + (r_{i+1} - r_i)^2] / 2 \}^{1/2}) / \mu_i \quad (5)$$

246 In addition, to classify the risk of aggressiveness of rainfall we propose a synthetic
247 parameter called *Annual Aggressiveness Risk* (R_A), derived from the indicators explained
248 above

$$249 \quad R_A = f(I_{FM}, I_{PC}) \quad (6)$$

250 The R_A parameter has the advantage of unifying all the information, so as to allow a more
251 concise interpretation of the rainfall impacts. The function f may be determined locally
252 based on erosivity data measured during the simultaneous period with high frequency
253 registers. For this, the R factor rainfall erosivity of the Universal Soil Loss Equation (USLE)
254 is used. Thus, this procedure connects methods based on monthly data with intra-hour data
255 analysis methods. In each case, the function f allows both the extrapolation into the past and
256 the analysis of the evolution of aggressiveness in historical periods. We have used this
257 methodology to analyze the aggressivity for each basin and to compare their behaviour on
258 an interregional scale. However, because this methodological approach involves the regional
259 aggregation of the precipitation data, the variations on shorter distances (intra-basins) have
260 not been analyzed in this study. Additionally this methodology can also be applied to
261 selected meteorological stations in every basin and then to establish spatial patterns within
262 them.

263 **4. Results and assessment**

264 The annual series of the Modified Fournier Index and the Precipitation Concentration Index
265 were calculated for each zone from precipitation datasets. In section 4.1 we present a general
266 characterization of the I_{FM} series. In section 4.2 the temporal evolution is analysed in detail.
267 Subsequently, a similar procedure was carried out for the I_{PC} series (described in sections
268 4.3 and 4.4). Finally, the joint interpretation of both indicators (4.5) and the analysis of the
269 risk of aggressiveness (4.6) were implemented.

270 *4.1. Characterization of the Modified Fournier Index (I_{FM})*

271 The results of the temporal analysis of the complete series of the variable I_{FM} in each zone
 272 are displayed in Table 1. The order of the zones corresponds to the organization of
 273 watersheds explained in section 2. For the analyzed period (1941 to 2010) the mean value,
 274 the coefficient of linear trend, the coefficient of variation (V_N) and the general disparity
 275 index (I_D) are shown.

276 *Table 1 around here*

277 It is important to highlight that the Modified Fournier Index result is high ($I_{FM} > 120 \text{ l/m}^2$) in
 278 the Cantabrian, Galicia and Guadalquivir zones, coinciding with the highest annual rainfall.
 279 It is moderate ($I_{FM} < 90 \text{ l/m}^2$) in other zones. These results confirm that I_{FM} is highly
 280 influenced by total annual rainfall, masking intense rain events of shorter duration.

281 The trend lines of the annual series show a slight up- or down-slope, but they are not
 282 statistically significant since the variance explained by the trend line is in all cases less than
 283 one percent ($R^2 < 0.1$). Therefore, the central value is not a good predictor of the temporal
 284 behaviour of rainfall aggressiveness. However, the cumulative relative deviations A_k , permit
 285 the distinction of multiannual sequences of different climatic behaviours. The cumulative
 286 value until the year k is obtained as the sum, extended to all preceding years, of the
 287 deviations δ_i of each annual index I_{FMi} from the mean μ_N of the entire series.

$$288 \quad A_k = (\sum \delta_i) / \mu_N \quad (7)$$

289 where $\delta_i = (I_{FMi} - \mu_N)$, for $i = 1, 2, \dots, k; k \leq N$.

290 Fig. 2 shows the annual accumulation of the relative deviations from the mean of the I_{FM} in
 291 each zone during the period 1941–2010. The sawtooth of the horizontal sections of the
 292 graph (Fig. 2) indicate multiannual sequences of the values of the I_{FM} where deviations by
 293 excess and by deficit from the mean compensate. The descending [ascending] section is due
 294 to multi-year sequences with higher frequency of values of lower [higher] I_{FM} than the mean
 295 of the entire series.

296

Fig. 2 around here

297 Interestingly, all the analysed areas show an initial downward segment – with the sawtooth –
298 resulting from the increased frequency of I_{FMF} values below the average; in 1958 the trend
299 changes with an upward section (high values of I_{FM}) of different duration for each zone. In
300 particular, the Cantabrian zone (Fig. 2a) shows a long upward section after 1958 until 1984,
301 when the direction changes again. The Atlantic watershed zones (Galicia, Douro, Tagus,
302 Guadiana and Guadalquivir zones: Figs. 2a, 2b and 2c) show matching profile graphics with
303 a concurrence in the sawteeth, including the secondary minimum in 1995. All this denotes a
304 common temporal pattern. The profiles of the Southeastern and Jucar zones (Fig. 2d) and the
305 Ebro and Catalanian zones (Fig. 2e) also match. In the last thirty years there have been some
306 zones (Ebro, Guadalquivir, Guadiana, Douro) whose annual I_{FM} values have fluctuated
307 around their averages values (horizontal section). However, the other zones show a final
308 section, as a result of repeated sequential years with I_{FM} values lower than the mean of the
309 series in the last decades. We can say that initially all zones show a similar temporal
310 behavior of their I_{FM} , with V-shaped graphs from 1941 to 1971 with their vertices in 1958,
311 but in recent decades that analogy does not hold. Anyhow, it is noteworthy that 1958 is
312 singular in the whole Peninsula, when a sequence break occurs.

313 Table 1 also shows the general irregularity of I_{FM} in each zone during the entire period from
314 1940 to 2010. Both the measure of variability V_N and disparity I_D reveal similarities between
315 both statistics in their geographical distribution. The irregularity is low in the Cantabrian
316 zone, indicating slight fluctuations of the annual I_{FM} value over time. In the Atlantic zones
317 there is a south–north gradient and the Guadalquivir zone shows the largest amplitude in
318 annual deviations of I_{FM} to the mean value (V_N) and to the successive values (I_D). From the
319 interpretation of the characteristic I_{FM} value (first column of Table 1) and its irregularity
320 (third and fourth columns of Table 1) we can deduce that the Cantabrian zone maintains

321 stability in its high potential rainfall aggressiveness; in the Guadalquivir zone, the potential
322 aggressiveness is high although the annual values are unstable, and in the Ebro the potential
323 rainfall aggressiveness is low and the annual values are steady.

324 It is important to note that in the context of the whole Iberian Peninsula, the Mediterranean
325 zones do not show the largest interannual irregularities in their I_{FM} indices. This is because,
326 although locally intense rainfall events occur occasionally (Martin-Vide, 2004; Rodrigo
327 2010), they do not alter the permanent shortage of total annual rainfall on a basin scale.
328 Consequently, except in the mountains or in the irrigated meadows, the main environmental
329 feature of large areas of the Mediterranean basin is aridity.

330 For further comparison of the temporal behaviour during the study period, we used the
331 Pearson Correlation Coefficient R between the annual series of I_{FM} of the delimited zones
332 (Table 2). This allowed us to quantify the extent to which the zones have followed a similar
333 development.

334 *Table 2 around here*

335 We can deduce (Table 2) that the interannual correspondence of the I_{FM} between the Plateau
336 zones (Douro, Tagus, Guadiana) is very high (≥ 0.80) and it is slightly lower than that of the
337 rest of the Atlantic zones (Guadalquivir and Galicia). In the Atlantic watershed the temporal
338 variations of the Modified Fournier Index maintained relative simultaneity. In the
339 Mediterranean zones a northeast gradient is observed. Except for the neighboring Ebro and
340 Galicia zones, the correlation between the Cantabrian and the other case study areas is very
341 low (≤ 0.20), indicating the different synoptic conditions that lead to precipitation in their
342 respective watersheds.

343 *4.2. Specific irregularity of the Modified Fournier Index*

344 In each zone the foregoing characterization of the annual series of the I_{FM} during the entire
345 period is complemented with the analysis of the specific interannual irregularity. For this,

346 the mobile variation coefficient using periods of eleven years V_{11} was calculated as a first
347 step (Fig. 3).

348

Fig. 3 around here

349 In the Cantabrian area the coefficient of variation V_{11} shows a decreasing profile from 0.20
350 to 0.10 during the observation period, indicating a progressive interannual stabilization of
351 the I_{FM} index in recent decades. The graph for Galicia shows a succession of multiannual
352 horizontal sections at different levels, framed between 0.25 and 0.35. A marked increase in
353 the variability of the I_{FM} in the Guadalquivir zone is detected from 1980, when V_{11} goes
354 from 0.30 to values above 0.50, and then finally a decline in the last decade; with less
355 intensity, mostly from 0.20 to 0.30, the Plateau zones (Guadiana and Tagus) also exhibit
356 similar behaviour. In Jucar and in the Southeastern zones during 1960–1980 and in the Ebro
357 during the whole period analysed, the coefficient of variation V_{11} is limited between 0.10
358 and 0.25, suggesting slight interannual oscillations of the I_{FM} around its central value.

359 The irregularity of the time series of the I_{FM} index analysed using their variability is also
360 reflected when using specific disparity as a criterion for study. This parameter indicates the
361 amplitude of the difference between consecutive years (Fig 4). The annual index of disparity
362 I_{di} shows a great simultaneity in behaviour between the Guadalquivir zone and the Plateau
363 zones (Fig. 4a; to provide a better visualization, the Plateau zones have been grouped by
364 their similar behaviour). These hydrological zones show their highest frequencies in the
365 range from 0.30 to 0.40 and it shows that their relative maxima show a strong positive trend
366 from 1971 to 1995. In the Ebro zone the I_{di} index, with marked fluctuations, maintains
367 frequent values near to 0.15, whilst other Mediterranean basins oscillate more slightly
368 around 0.3 (Fig. 4b). Due to their geographical proximity, the profile of the disparity in the
369 Cantabrian zone (descending and with smooth fluctuations) contrasts with the one for
370 Galicia (ascending and with wide fluctuations) (Fig. 4c).

371

Fig. 4 around here

372 4.3. Characterization of the Precipitation Concentration Index I_{PC}

373 As we have pointed out, in some situations the Modified Fournier Index I_{FM} does not evince
374 the effect of the intra-annual distribution. Therefore, estimating aggressiveness is
375 complemented by the calculation of the Precipitation Concentration Index I_{PC} based on the
376 same data. Oliver (1980) established the classification under which I_{PC} values below 10
377 represent sparse rainfall throughout the year (uniform equipartition of rainfall throughout
378 every month of the year is the minimum value 8.3); I_{PC} values over 15 indicate concentrated
379 rainfall (more than 60% of the total annual rainfall occurs in only four months).

380

Table 3 around here

381 The averages of the concentration index in the zones of the southern half of the Peninsula
382 are higher than in the northern half (Table 3). The south–north gradient of I_{PC} is observed in
383 both the Atlantic and the Mediterranean watersheds. The highest frequencies of years with
384 high intra-annual concentration values, $I_{PC} \geq 15$ and with marked seasonality are found in
385 the southern areas: the Guadalquivir zone (55%) and the Southeastern zone (34%).
386 However, the northern zones show the highest frequency of years with high dispersion
387 throughout the year ($I_{PC} \leq 10$), specifically the Ebro zone (40%) followed by the Cantabrian
388 zone (14%).

389 Table 3 also shows that the slope of the trend line of the annual series for the entire period of
390 analysis is very low and not statistically significant in any of the zones. It also states that the
391 general irregularity of the I_{PC} in the comparison between zones shows similar features for
392 the entire period 1940–2010 in terms of variability V_N and disparity I_D . The I_{PC}
393 concentration index shows low variability in the northern peninsula, in the Cantabrian ($V_N =$
394 0.09) and the Ebro zones ($V_N = 0.10$), compared to the Southeastern ($V_N = 0.14$), the Tagus
395 ($V_N = 0.17$), the Guadiana ($V_N = 0.17$) and, especially, the Guadalquivir zones ($V_N = 0.19$). A

396 similar spatial relationship is observed in the values of the general disparity I_D during the
397 period 1941–2010.

398 The analysis of cumulative deviations of the I_{PC} during this period allows temporal
399 sequences to be detected. Fig. 5 shows that the years 1958 and 1978 have a singular
400 behaviour because they represent breaks in time sequences. In the graph for the Jucar zone
401 and the Southeastern zone (Fig. 5d) this is clearly visible, but it can be extended to the other
402 cases studied. A section where there is a downward trend with frequencies of years in which
403 the I_{PC} value is lower than the average, and therefore where there is more concentration
404 around the winter months, ends in 1958. Except in the Catalanian zone, a new upward
405 section starts in 1978 (Fig. 5e), suggesting greater intra-annual dispersion with shifts of the
406 periods of rainfall to autumn and/or spring.

407 *Fig. 5 around here*

408 We have indicated that the Pearson Correlation Coefficient R between the annual series
409 permits comparisons of the extent to which they have followed similar trends over the entire
410 period from 1941 to 2010. The results in Table 4 reveal that the interannual I_{PC}
411 correspondence is negligible between the Catalanian zone and the remainder ($R < |0.2|$),
412 except for Jucar and Ebro. However, it is high among the zones of the Plateau with each
413 other and with the Guadalquivir zone ($R > 0.6$), indicating simultaneity between the zones of
414 the Atlantic watershed during the years of greatest concentration and also during the years of
415 highest intra-annual dispersion.

416 *Table 4 around here*

417 4.4. Specific irregularity of the Precipitation Concentration Index I_{PC}

418 A space-time analysis of the specific interannual irregularity of the Concentration Index I_{PC}
419 was performed using a similar approach to that used in Section 4.2. With this aim, we
420 calculated the mobile coefficient of variation using periods of eleven years V_{11} whose partial

421 results are shown in the Supplementary Electronic Material (from now ESM) Figure ESM-1.
422 The area of Cantabria and the Ebro river show, in general, the least variability of I_{PC} , with
423 the particularity of presenting an opposite behavior since 1964. The area of the Guadalquivir
424 river presents the greatest variability of I_{PC} . The graphs of the southeast and the Júcar river
425 areas show very similar profiles. Therefore, there is an uniform spatial pattern that can
426 describe the specific interannual variability of I_{PC} in the Iberian Peninsula, except between
427 the neighboring areas of the same basin.

428 Among the results of the specific disparity I_d of the I_{PC} index we have selected the most
429 significant ones, which are those for Tagus/Guadiana and Galicia/Ebro basins (Fig. 6). It is
430 important to note the temporal simultaneity reflected in the overlay profiles of the chosen
431 zones, Tagus and Guadiana (Fig. 6a), are to a large degree coincident with the temporal
432 evolution of Guadalquivir (not shown). In them, the relative maxima show an upward
433 alignment in recent decades. This implies an increase in the range of intra-annual dispersion
434 of rainfall in consecutive years. In the Galicia and the Ebro zones the time series reflects a
435 decline in relative maxima, without concurrency, until 1970 (Fig. 6b). From that year, in the
436 Ebro zone the maxima increase progressively, while in Galicia, after a sharp rise, the values
437 tend to decrease again.

438 *Fig. 6 around here*

439 *4.5. Comparison between the temporal evolution of the indices I_{FM} and I_{PC}*

440 The joint interpretation of the temporal behaviour of the Modified Fournier Index (I_{FM}) and
441 the Precipitation Concentration Index (I_{PC}) can be used to estimate the rainfall
442 aggressiveness more accurately. Thereby, simultaneous high values of both annual indices
443 correspond to high risk: high annual rainfall and very seasonally concentrated. In contrast,
444 the simultaneous low values of both indices indicate relatively dry years but well-distributed
445 rainfall throughout the year. Therefore, for the whole period of analysis, the association of

446 pairs of values have been established for each year and zone. Fig. 7 shows the range width
447 for both indices, the equation of the trend line and the Pearson coefficient of determination
448 (R^2) calculated for the period from 1941 to 2010. For graphical representation we have
449 chosen the following zones: Cantabrian (north)/Guadalquivir (southwest), Galicia
450 (northwest)/Jucar (east), Ebro (northeast)/Guadiana (west), facilitating the visualization of
451 the different rainfall patterns in the Iberian Peninsula.

452 Fig. 7 reveals that the range of values of both indices provides an identification of the zones.
453 In all the zones the coefficient of the line is positive, suggesting that high/low annual values
454 are associated with high values of I_{PC} , although with different statistical significance.
455 However, the observed values of the determination coefficient R^2 below 0.5 are not enough
456 to deduce that generally the wettest years (high I_{FM}) are due to excess rainfall concentrated
457 in certain months (high I_{PC}). Although the trend lines are parallel (linear coefficient of 9.76
458 and 9.08, respectively) the range of the I_{PC} marks a difference between the Cantabrian zone
459 and the Guadalquivir zone (Fig. 7a). In the Cantabrian zone, without large interannual
460 fluctuations, there are frequently years when the intra-annual distribution of rainfall is very
461 distributed throughout the months ($I_{PC} < 12$). In Andalusia (Guadalquivir), there is a great
462 temporal diversity of both I_{FM} and I_{PC} indices, but years of intense seasonality ($I_{PC} < 15$) are
463 frequent, which is associated with intra-annual unimodal distribution with a maximum in
464 winter (García-Barrón et al., 2010).

465 In Galicia and Jucar the intra-annual distribution is similar between the two zones ($10 < I_{PC}$
466 < 15) for all the years studied (Fig. 7b). However, the I_{FM} is higher in Galicia, which may be
467 due to its greater total annual rainfall compared to the Jucar zone, with less annual
468 precipitation and less interannual variability ($I_{FM} < 100 \text{ l/m}^2$).

469 Ebro shows $I_{PC} < 12$ values, associated with a bimodal intra-annual distribution profile with
470 maxima of rainfall in spring and autumn and a relative minimum in winter (García-Barrón et

471 al., 2010). In Guadiana the I_{FM} shows a wide range of values associated with the irregularity
472 of the interannual precipitation resulting in dry years and wet years (similar to Guadalquivir
473 but less intense) and also a wide range of I_{PC} ($10 < I_{PC} < 20$) corresponding to a large intra-
474 annual variability (Fig. 7c).

475 *Fig. 7 around here*

476 The above results are justified by the precipitation regime in each zone. The storms of the
477 SW and those of the NW, which are less intense, determine the rainfall of the Spanish
478 Atlantic watershed, mainly in the zones of Guadalquivir and Galicia, although they slightly
479 diminish in the Plateau zones (Douro, Tagus, Guadiana) because of the effect of
480 continentality due to the greater distance from the sea. The influence of the Azores High,
481 located southwest of Portugal for much of the year, limits the approach of SW storms which
482 are deflected to northern regions. This also explains the gradient between the southwest and
483 northwest in the Peninsula: the highest rainfall is more evenly distributed in Galicia, the
484 same north–south effect, but more attenuated, occurs between the zones of the Plateau as
485 well.

486 In the Mediterranean watershed, the difficulty the Atlantic winds have in reaching the
487 headwaters and the proximity to the Mediterranean Sea (with factors related to seasonal
488 atmospheric circulation in autumn and the wet influences from the northeast) make a
489 difference to the rainfall regime compared to the Plateau. In the Cantabrian watershed, the
490 narrow coastal strip (defined by the altitude of the next ridge that holds the flow of moisture
491 and prevents its transition to the Plateau) receives heavy rainfall, with weak seasonality, due
492 to the presence of the NW Atlantic fronts for much of the year. The Ebro zone also presents
493 weather oddities in comparison to the Iberian Peninsula, mainly due to the water coming
494 from the southern slopes of the Pyrenees, the isolation of the Plateau by the Iberian System

495 mountain range and the connection between the influences of the Cantabrian and the
496 Mediterranean Seas along the axis of the Ebro river basin.

497 *4.6 Risk of aggressiveness of rainfall in the Guadalquivir zone*

498 To classify the risk of rainfall aggressiveness, the R_A parameter, which summarizes the
499 information provided by I_{FM} and I_{PC} , is proposed. A new series of annual risk of
500 aggressiveness in the Guadalquivir zone was generated according to the procedure described
501 in section 3.

502 In order to establish the weights of both the I_{FM} and I_{PC} components, two values have been
503 chosen for the R erosivity factor calculated by the Andalusian Environment Information
504 Network for the Guadalquivir river basin. This network provides monthly values of rainfall
505 erosivity between 1991 and 2010 for the area, taking in account the rainfall data collected by
506 the automatic weather stations. These values are determined by the regionalization of
507 Andalusia based on the delimitation of homogeneous rainfall zones according to the rainfall
508 intensity parameter. After that, for each of these regions one or more weather stations with
509 high frequency records were selected and the regression equation between their R factor
510 values and their total annual rainfall was calculated (Rodríguez Surián and Sánchez Pérez,
511 1995). The best-fit model has the form $y = a \chi^b$ (where a and b are local parameters)
512 implemented on decadal total rainfall and giving coefficients of determination R^2 above
513 0.90.

514 Throughout the simultaneity period, the correlation coefficient between the erosivity R
515 factor and the Modified Fournier Index (I_{FM}) is 0.9, and between R factor and the
516 Precipitation Concentration Index (I_{PC}) is 0.55. Although it cannot be generalized to other
517 geographic areas, it is important to highlight the high capacity of the I_{FM} Index to predict the
518 aggressiveness impact. If we consider the two indices jointly, the fit equation estimated by
519 multiple linear regression is

520
$$R = R_A + \xi ; R_A = 11.32 I_{FM} - 61.6 I_{PC} + 663.3 \quad (8)$$

521 where ξ is a residual value of mean equal to zero.

522 Applying the equation to every year of the concurrency period we obtain the theoretical
523 value of R_A as opposed to the reference value of R . Fig. 8 shows both series, whose high
524 correspondence (correlation coefficient $R^2 > 0.88$) supports the validity of the procedure.

525 *Fig. 8 around here*

526 When extrapolating into the past, we have generated the series for the interannual
527 aggressiveness risk in the Guadalquivir river basin during the period 1941–2010 from the
528 values of I_{FM} and I_{PC} . The R_A series with an average value of 1909.3 (Megajoules ·
529 mm)/(hectare · year · hour) reveals no significant trend and is characterized by its high
530 irregularity with a coefficient of variation (CV) of 0.41. Figure ESM-2 shows the time
531 evolution of R_A . Years with values below the 25 percentile ($R_A < 696.8$) are considered years
532 with low aggressiveness risk, while those over the 75 percentile (R_A values > 1273.4) are
533 classified as high risk.

534 We consider the procedure for calculating the aggressiveness risk R_A in the long-term time
535 series as a useful method for analysing the environmental impact. In future work the
536 research team plans to apply the procedure to a set of automatic weather stations in
537 Andalusia that maintain secular records of monthly precipitation.

538 **5. Conclusions**

539 The advantage of the methodology used, based on information provided by the SIMPA
540 model, is that it provides series of environmental indicators for extended multi-year periods,
541 representative of large areas, where extreme local values are damped. This allows the
542 analysis, from a space-time approach, of the effects of rainfall over the entire Iberian
543 Peninsula. The procedure for calculating the rainfall aggressiveness uses the Modified
544 Fournier Index (I_{FM}) in conjunction with the Precipitation Concentration Index (I_{PC}), both

545 based on monthly rainfall data. These indices – and their relationship to the spatial and
546 temporal distribution of rainfall aggressiveness and its environmental effects – have enabled
547 patterns to be studied associated with rainfall and its temporal variability (Apaydin et al.,
548 2006). Therefore, the development and application of methodologies and analysis, such as
549 those proposed for observing the patterns of interannual variability by these indices and their
550 differential behaviour through case studies, are important in supporting the understanding
551 the functioning of the socio-hydrological systems.

552 During the analysis period (1940–2010) the potential rainfall aggressiveness measured with
553 I_{FM} is moderate in the Mediterranean Ebro and Plateau zones, and intense in the
554 Guadalquivir, Galicia and Cantabrian zones. The I_{FM} and I_{PC} series do not show a significant
555 linear trend over the entire period analysed, although several differentiated multiyear
556 sequences can be identified. An interannual correspondence between the I_{FM} values of the
557 Guadalquivir and the values of the Plateau zones and also between the Mediterranean zones
558 together is detected, but it is very low between the Cantabrian and other zones, indicating
559 differences in rainfall patterns. The largest interannual irregularity of aggressiveness, as
560 measured by the variability and disparity of the I_{FM} series, occurs in the Guadalquivir zone;
561 the basins of the Plateau show a simultaneous temporal development, although it is less
562 intense. In addition, an increase in temporal variability in Guadalquivir can be detected over
563 the last thirty years. By contrast, the Cantabrian zone presents the greatest stability in its
564 time series with smooth fluctuations, although increasing over time.

565 The interpretation of the Concentration Index I_{PC} indicates that, although not uniformly, the
566 rainfall in the Cantabrian and the Ebro zones is distributed throughout the year without
567 excessive interannual oscillations. Therefore, in these zones the main feature is the
568 interannual and intra-annual stability. However, both the Atlantic and the Mediterranean
569 watersheds show a north–south gradient in their I_{PC} , so that in the Guadalquivir rainfall is

570 highly seasonal and it is mainly concentrated in just a few months, with large interannual
571 fluctuations. These large fluctuations are embodied in intra-annual rainfall concentration
572 values that are changing over time, showing a north–south spatial pattern where interannual
573 and intra-annual instability increases with decreasing latitude. In these areas this
574 phenomenon can help to complement the study of the relationship between the processes of
575 seasonality/concentration of rainfall and of factors controlling the seasonal dynamics of
576 vegetation in the Mediterranean areas, where the intra-annual distribution of rainfall
577 amounts and the response of vegetation cover involve differences in the processes of
578 erosivity, soil instability and desertification on a larger scale.

579 Finally, a general pattern of rainfall aggressiveness in the Iberian Peninsula under a dual
580 effect is shown: the effect of latitude, with a north–south increase in the irregularity of the
581 indices studied; and the effect of longitude, marked by the different maritime influences on
582 the Atlantic and Mediterranean watersheds. The space-time variability identified should be
583 compared to other regional studies related to the assessment of the impact and vegetative
584 response to seasonal rainfall in terms of vegetation cover in order to determine trends in the
585 relationship of precipitation (vegetative response) and environmental risk in the context of
586 climate change.

587 From the Modified Fournier index (I_{FM}) and the Concentration Index (I_{PC}), we calculated the
588 risk of rainfall aggressiveness R_A . The first partial results obtained allow the risk of
589 aggressiveness to be estimated, based on monthly rainfall records, which can connect with
590 other indicators based on high-frequency records. This opens the possibility of its
591 application in future research.

592 Preliminary results in the Guadalquivir river basin support the predictive ability of the
593 aggressiveness risk R_A ; future studies may reveal its utility to determine environmental
594 impacts in other river basins.

595 **Acknowledgements**

596 This study was partially funded by the Project 158-2010 (Autonomic Agency of National
597 Parks) of the Ministry of Environment and by the National Plan of Research and
598 Development of the Ministry of Education and Science (Project CGL2009-10683). We also
599 thank the Ministry of Environment of the Junta de Andalucía which has provided the data
600 for erosivity in the Guadalquivir river basin, as well as the feedback from reviewers and
601 editors of this MS to improve its content.

602 **Appendix A. Supplementary material**

603 Supplementary data associated with this article can be found, in the online version.

604 **References**

- 605 Acero, F.J., Gallego, M.C., García J.A., 2011. Multi-day rainfall trends over the Iberian
606 Peninsula. *Theoretical and Applied Climatology* 108 (3–4), 411–423.
- 607 Angulo-Martínez, M., López-Vicente, M., Vicente-Serrano, S.M., Beguería, S., 2009.
608 Mapping rainfall erosivity at a regional scale, a comparison of interpolation methods
609 in the Ebro Basin (NE Spain). *Hydrology and Earth Systems Science* 13, 1907–1920.
- 610 Apaydin, H., Erpul, G., Bayramin, I., Gabriels, D., 2006. Evaluation of indices for
611 characterizing the distribution and concentration of precipitation: A case for the
612 region of Southeastern Anatolia Project, Turkey. *Journal of Hydrology* 328 (3), 726–
613 732.
- 614 Arnoldus, H.M.J., 1980. An approximation of the rainfall factor in the universal soil loss
615 equation, in: De Boodt, M., Gabriels, D. (Eds.), *Assessment of Erosion*. John Wiley,
616 Chichester, pp. 127–132.
- 617 Barriandos, M., Rodrigo, F.S., 2006. Study of historical flood events on Spanish rivers using
618 documentary data. *Hydrological Sciences Journal* 51 (5), 765–783.

619 Bejarano, M.D., Marchamalo, M., de Jalón, D.G., Tánago, M.G., 2010. Flow regime
620 patterns and their controlling factors in the Ebro basin (Spain). *Journal of Hydrology*
621 385 (1), 323–335.

622 Belmar, O., Velasco, J., Martínez-Capel, F., 2011. Hydrological classification of natural flow
623 regimes to support environmental flow assessments in intensively regulated
624 Mediterranean Rivers, Segura River Basin (Spain). *Environmental Management* 47
625 (5), 992–1004.

626 Briggs, D., Giordano, A., Cornaert, M., Peter, D., Maef, J., 1992. Commission of the
627 European Communities, 1992. CORINE soil erosion risk and important land
628 resources in the southern regions of the European Community. Commission of the
629 European Communities Publication, EUR, 13233, Luxembourg.

630 Caramelo, L., Manso-Orgaz M.D., 2007. A study of precipitation variability in the Duero
631 Basin (Iberian Peninsula). *International Journal of Climatology* 27 (3), 327–339.

632 Chavez-Jimenez, A., Lama, B., Garrote, L., Martín-Carrasco, F., Sordo-Ward, A., Mediero,
633 L., 2013. Characterisation of the sensitivity of water resources systems to climate
634 change. *Water Resources Management* 27 (12), 4237–4258.

635 Costa, A.C., Santos, J.A., Pinto, J.G., 2012. Climate change scenarios for precipitation
636 extremes in Portugal. *Theoretical and Applied Climatology* 108 (1–2), 217–234.

637 Da Silva A.M., 2004. Rainfall erosivity map for Brazil. *Catena* 57 (3), 251–259.

638 De Castro, M., Martín-Vide, J., Alonso, S., 2005. El clima de España: Pasado, presente y
639 escenarios de clima para el siglo XXI. Ministerio de Medio Ambiente, Madrid.

640 De Luis, M., Brunetti, M., González-Hidalgo, J.C., Longares, L.A., Martín-Vide, J., 2010a.
641 Changes in seasonal precipitation in the Iberian Peninsula during 1946–2005. *Global
642 and Planetary Change* 74 (1), 27–33.

- 643 De Luis, M., Gonzalez-Hidalgo, J.C., Longares L.A., 2010b. Is rainfall erosivity increasing
644 in the Mediterranean Iberian Peninsula? *Land Degradation & Development* 21 (2),
645 139–144.
- 646 De Luis, M., González-Hidalgo, J.C., Brunetti, M., Longares, L.A., 2011. Precipitation
647 concentration changes in Spain 1946–2005. *Natural Hazards and Earth System*
648 *Science* 11 (5), 1259–1265.
- 649 De Vente, J., Poesen, J., Verstraeten, G., Van Rompaey, A., Govers, G., 2008. Spatially
650 distributed modelling of soil erosion and sediment yield at regional scales in Spain.
651 *Global and Planetary Change* 60 (3), 393–415.
- 652 Del Rio, S.D., Herrero L., Fraile R., Penas, A., 2011. Spatial distribution of recent rainfall
653 trends in Spain (1961–2006). *International Journal of Climatology* 31 (5), 656–667.
- 654 Dima, M., Lohmann, G., Dima I., 2005. Solar-induced and internal climate variability at
655 decadal time scales. *International Journal of Climatology* 25 (6), 713–733.
- 656 Diodato, N., Knight J., Bellocchi G., 2013. Reduced complexity model for assessing
657 patterns of rainfall erosivity in Africa. *Global and Planetary Change* 100, 183–193.
- 658 Diodato, N., Bellocchi, G., 2007. Estimating monthly (R)USLE climate input in
659 Mediterranean region using limited data. *Journal of Hydrology* 345 (3), 224–236.
- 660 Diodato, N., Bellocchi, G., Romano, N., Chirico, G.B., 2011. How the aggressiveness of
661 rainfalls in the Mediterranean lands is enhanced by climate change. *Climatic Change*
662 108 (3), 591–599.
- 663 Do Ó, A., 2010. Transboundary drought risk management in Mediterranean Europe: A state-
664 of-the-art analysis for the Guadiana River Basin. *Options Méditerranéennes* 95 (A),
665 267–272.
- 666 Elagib, N.A., 2011. Changing rainfall, seasonality and erosivity in the hyper-arid zone of
667 Sudan. *Land Degradation & Development* 22 (6), 505–512.

668 Embid, A., Gurrea, F., 2004. Relevance and application of the EU water directive in terms
669 of Spain's National Hydrological Plan. *Water Science & Technology* 49 (7), 111–
670 116.

671 Estrela, T., Pérez-Martín, M.A., Vargas, E., 2012. Impacts of climate change on water
672 resources in Spain. *Hydrological Sciences Journal* 57 (6), 1154–1167.

673 Estrela, T., Quintas, L., 1996. El sistema integrado de modelización precipitación-aportación
674 SIMPA. *Ingeniería Civil* 104, 43–52.

675 Estrela, T., Cabezas, F., Estrada, F., 1999. La evaluación de los recursos hídricos en El libro
676 blanco del agua en España. *Ingeniería del Agua* 6 (2), 125-138.

677 Febles, J.M., Tolón, A., Vega, M.B., 2009. Edaphic indicators for assesment of soil erosion
678 in karst regions, province of Havana, Cuba. *Land Degradation & Development* 20
679 (5), 522–534.

680 Fournier, F., 1960. *Climat et érosion*. Presse Universitaire de France, Paris.

681 Gabriels, D., 2006. Assessing the modified Fournier Index and the Precipitation
682 Concentration Index for some European countries, in: Boardman, J., Poesen, J.
683 (Eds.), *Soil Erosion in Europe*. John Wiley & sons, Chichester, pp. 675–684.

684 García, J.A., Gallego, M.C., Serrano, A., Vaquero J.M., 2007. Trends in block-seasonal
685 extreme rainfall over the Iberian Peninsula in the second half of the twentieth
686 century. *Journal of Climate* 20 (1), 113–130.

687 García-Barrón, L., Camarillo, J.M., Morales, J., Sousa, A., 2010. Caracterización
688 pluviométrica intraanual de la Península Ibérica, in: Fernández, F., Galán, E.,
689 Cañada, R. (Eds.), *Publicaciones de la Asociación Española de Climatología A 7*,
690 Madrid, pp. 389–398.

691 García-Barrón, L., Aguilar, M., Sousa A., 2011. Evolution of annual rainfall irregularity in
692 the southwest of the Iberian Peninsula. *Theoretical and Applied Climatology* 103 (1–
693 2), 13–26.

694 García-Barrón, L., Morales, J., Sousa, A., 2013. Characterisation of the intra-annual rainfall
695 and its evolution (1837–2010) in the southwest of the Iberian Peninsula. *Theoretical*
696 *and Applied Climatology* 114 (3–4), 445–457.

697 Gonzalez-Hidalgo, J.C., Brunetti, M., de Luis, M., 2010. Precipitation trends in Spanish
698 hydrological divisions, 1946–2005. *Climate Research* 43 (3), 215–228.

699 Gregori, E., Andrenelli, M.C., Zorn, G., 2006. Assessment and classification of climatic
700 aggressiveness with regard to slope instability phenomena connected to hydrological
701 and morphological processes. *Journal of Hydrology* 329 (3), 489–499.

702 Kilsby, C.G., Tellier, S.S., Fowler, H.J., Howels, T. R., 2007. Hydrological impacts of
703 climate change on the Tejo and Guadiana Rivers. *Hydrology and Earth System*
704 *Sciences* 11 (3), 1175–1189.

705 Krysanova, V., Dickens, C., Timmerman, J., Varela-Ortega, C., Schlüter, M., Roest, K.,
706 Huntjens, P., Jaspers, F., Buiteveld, H., Moreno, E., Pedraza-Carrera, J., Slámová,
707 R., Martínková, M., Blanco, I., Esteve, P., Pringle, K., Pahl-Wostl, C., Kabat, P.,
708 2010. Cross-comparison of climate change adaptation strategies across large river
709 basins in Europe, Africa and Asia. *Water Resources Management* 24 (14), 4121–
710 4160.

711 Lee, J.H., Heo, J.H., 2011. Evaluation of estimation methods for rainfall erosivity based on
712 annual precipitation in Korea. *Journal of Hydrology* 409 (1), 30–48.

713 Lionello, P., Malanotte P., Boscolo, R., 2006. *Mediterranean climate variability*. Elsevier,
714 Amsterdam.

715 López-Moreno, J.I., Vicente-Serrano, S.M., Zabalza, J., Beguería, S., Lorenzo-Lacruz, J.,
716 Azorín-Molina, C., Morán-Tejeda, E., 2013. Hydrological response to climate
717 variability at different time scales: A study in the Ebro basin. *Journal of Hydrology*
718 477 (16), 175–188.

719 Lorenzo-Lacruz, J., Vicente-Serrano, S.M., López-Moreno J.I., Morán-Tejeda, E., Zabalza
720 J., 2012. Recent trends in Iberian streamflows (1945–2005). *Journal of Hydrology*
721 414–415, 463–475.

722 Machado, M.J., Benito, G., Barriendos, M., Rodrigo F.S., 2011. 500 Years of rainfall
723 variability and extreme hydrological events in southeastern Spain drylands. *Journal*
724 *of Arid Environments* 75 (12), 1244–1253.

725 Martín-Vide J., 2004. Spatial distribution of a daily precipitation concentration index in
726 peninsular Spain. *International Journal of Climatology* 24 (8), 959–971.

727 Martín-Vide, J., Olcina, J., 2001. *Climas y tiempos de España*. Alianza Editorial, Madrid.

728 Michiels, P., Gabriels, D., Hartmann, R., 1992. Using the seasonal and temporal
729 precipitation concentration index for characterizing monthly rainfall distribution in
730 Spain. *Catena*. 19 (1), 43–58.

731 Middelkoop, H., Daamen, K., Gellens, D., Grabs, W., Kwadijk, J.C.J, Lang, H., B.W.A.H.
732 Parmet, Schädler, B., Schulla, J., Wilke, K., 2001. Impact of climate change on
733 hydrological regimes and water resources management in the Rhine basin. *Climatic*
734 *change* 49 (1-2), 105-128.

735 MIMAM, 2000. *El Libro Blanco del Agua en España*. Ministerio de Medio Ambiente,
736 Madrid, Spain.

737 Ministerio de Agricultura, Alimentación y Medio Ambiente, 2013.
738 <http://servicios2.marm.es/sia/visualizacion/descargas/series.jsp>

739 Morán-Tejeda, E., López-Moreno J.I., Vicente-Serrano, S.M., Lorenzo-Lacruz, J., Ceballos-
740 Barbanchoa, A., 2012. The contrasted evolution of high and low flows and
741 precipitation indices in the Duero basin (Spain). *Hydrological Sciences Journal* 57
742 (4), 591–611.

743 Munka, C., Cruz, G., Caffera, R.M., 2007. Long term variation in rainfall erosivity in
744 Uruguay, a preliminary Fournier approach. *GeoJournal* 70 (4), 257–262.

745 Nippert, J.B., Knapp, A.K., Briggs, J.M., 2006. Intra-annual rainfall variability and
746 grassland productivity: Can the past predict the future? *Plant Ecology* 184 (1), 65–
747 74.

748 Oliver, J.E., 1980. Monthly precipitation distribution, a comparative index. *The Professional*
749 *Geographer* 32 (3), 300–309.

750 Pérez-Camacho, L., Salvador Rebollo, S., Hernández-Santana, V., García-Salgado, G.,
751 Pavón-García, J., Gómez-Sal, A., 2012. Plant functional trait responses to
752 interannual rainfall variability, summer drought and seasonal grazing in
753 Mediterranean herbaceous communities. *Functional Ecology* 26 (3), 740–749.

754 Rey, J.C., Rodríguez, M.F., Cortez, A., Lobo, D., Ovalles, F., Gabriels, D., Parra, R.M.,
755 2012. Analysis of precipitation aggressiveness and concentration in Venezuela. IV.
756 Los Andes Region. *Bioagro* 24 (2), 115-120.

757 Rodrigo F.S., 2010. Changes in the probability of extreme daily precipitation observed from
758 1951 to 2002 in the Iberian Peninsula. *International Journal of Climatology* 30 (10),
759 1512–1525.

760 Rodrigo, F.S., Trigo, R.M., 2007. Trends in daily rainfall in the Iberian Peninsula from 1951
761 to 2002. *International Journal of Climatology* 27 (4), 513–529.

762 Rodríguez Surián, M., Sánchez Pérez, J.D., 1995. Distribución espacio-temporal de las
763 pérdidas de suelo en Andalucía utilizando tecnología S.I.G. e imágenes de satélite.

764 http://www.juntadeandalucia.es/medioambiente/web/Red_informacion_ambiental/pr
765 [oductos/Publicaciones.](http://www.juntadeandalucia.es/medioambiente/web/Red_informacion_ambiental/pr)

766 Sánchez, E., Domínguez, M., Romera, R., López de la Franca N., Gaertner M.A., Gallardo,
767 C., Castro, M., 2011. Regional modeling of dry spells over the Iberian Peninsula for
768 present climate and climate change conditions. *Climatic Change* 107 (3–4), 625–634.

769 Sardans, J., Peñuelas, J., 2013. Plant-soil interactions in Mediterranean forest and
770 shrublands: Impacts of climatic change. *Plant and Soil* 365 (1–2), 1–33.

771 Sauerborn, P., Klein, A., Botschek, J., Skowronek, A., 1999. Future rainfall erosivity
772 derived from large-scale climate models-methods and scenarios for a humid region
773 *Geoderma* 93 (3), 269–276.

774 Sousa, A., García-Murillo, P., Sahin, S., Morales, J., García-Barrón, L., 2010. Wetland place
775 names as indicators of manifestations of recent climate change in SW Spain (Doñana
776 Natural Park). *Climatic Change* 100 (3–4), 525–557.

777 Sousa, A., Morales, J., García-Barrón, L., García-Murillo, P., 2013. Changes in the *Erica*
778 *ciliaris* Loeffl. ex L. peat bogs of southwestern Europe from the 17th to the 20th
779 centuries AD. *Holocene* 23 (2), 255–269.

780 Valencia, J.L, Tarquis, A.M., Saa-Requejo A., Gasco, J.M., 2012. Change of extreme
781 rainfall indexes at Ebro River Basin. *Natural Hazards and Earth System Science* 12
782 (7), 2127–2137.

783 Vicente-Serrano, S.M., 2006. Spatial and temporal analysis of droughts in the Iberian
784 Peninsula (1910–2000). *Hydrological Sciences Journal* 51 (1), 83–97.

785 Vrieling, A., Sterk, G., de Jong, S.M., 2010. Satellite-based estimation of rainfall erosivity
786 for Africa. *Journal of Hydrology* 395 (3), 235–241.

787

788 **Table captions**

789 **Table 1**

790 Characterization of the Modified Fournier Index (I_{FM}) in the Spanish zones defined from
791 1940 to 2010.

792 **Table 2**

793 Pearson correlation coefficient between the series of the Modified Fournier Index (I_{FM}) of
794 the case studies during the period 1940–2010.

795 **Table 3**

796 Characterization of the Precipitation Concentration Index (I_{PC}) in the Spanish zones defined
797 from 1940 to 2010.

798 **Table 4**

799 Pearson correlation coefficient between the series of the Precipitation Concentration Index
800 (I_{PC}) of the case studies during the period 1940–2010.

Figure 1 (colour)



Figure 2 (colour)

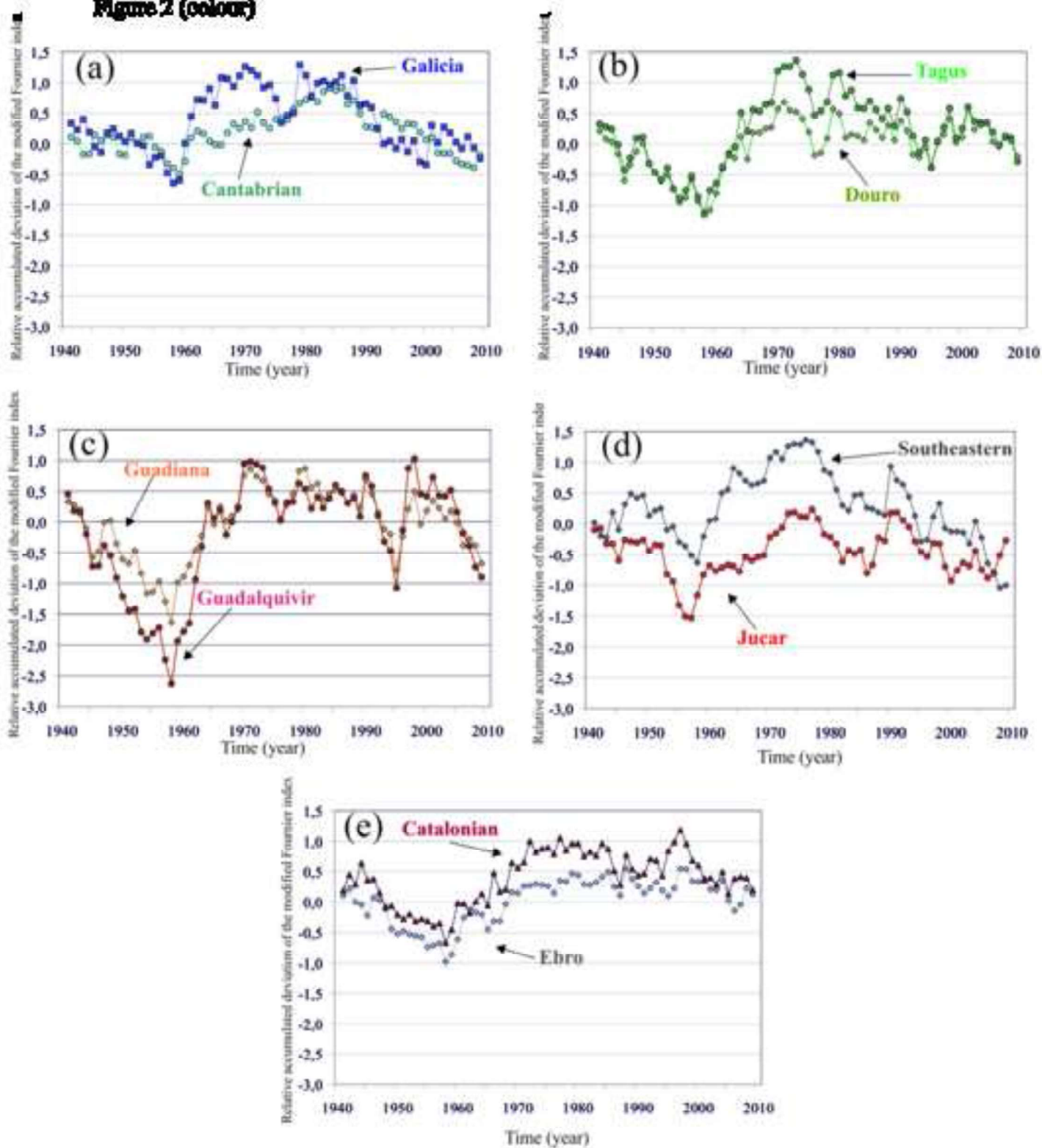


Figure
[Click here to download high resolution image](#)

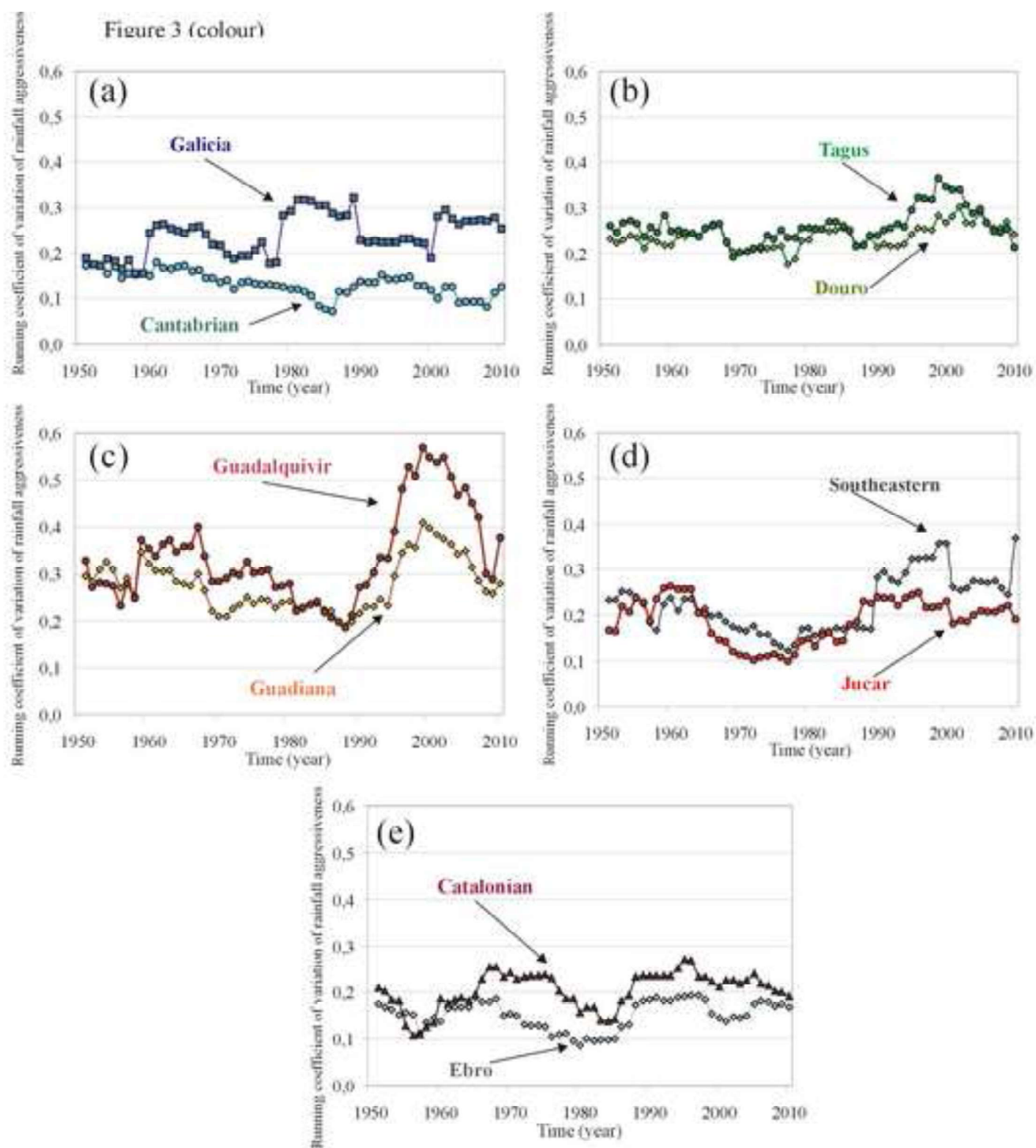


Figure 4 (colour)

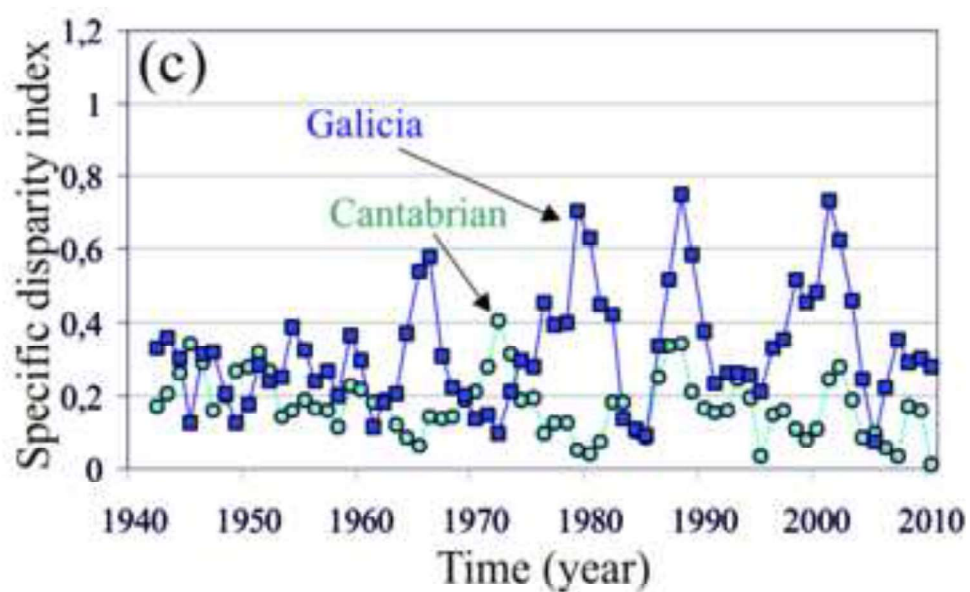
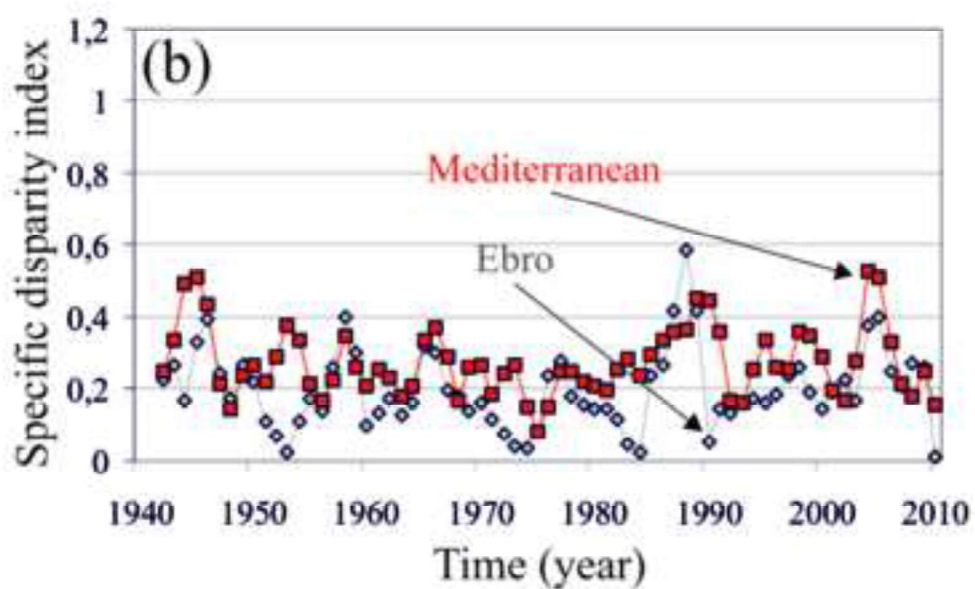
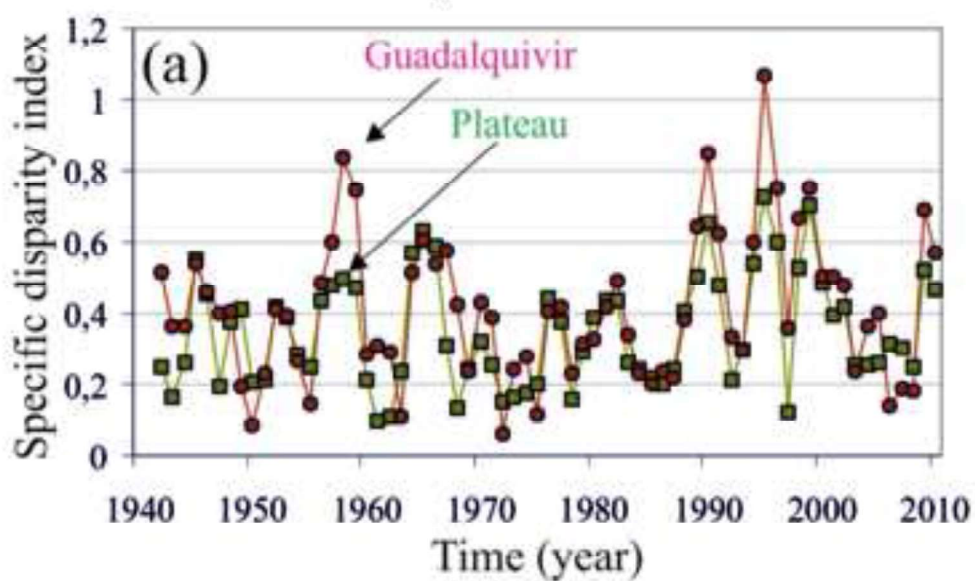


Figure 5 (colour)

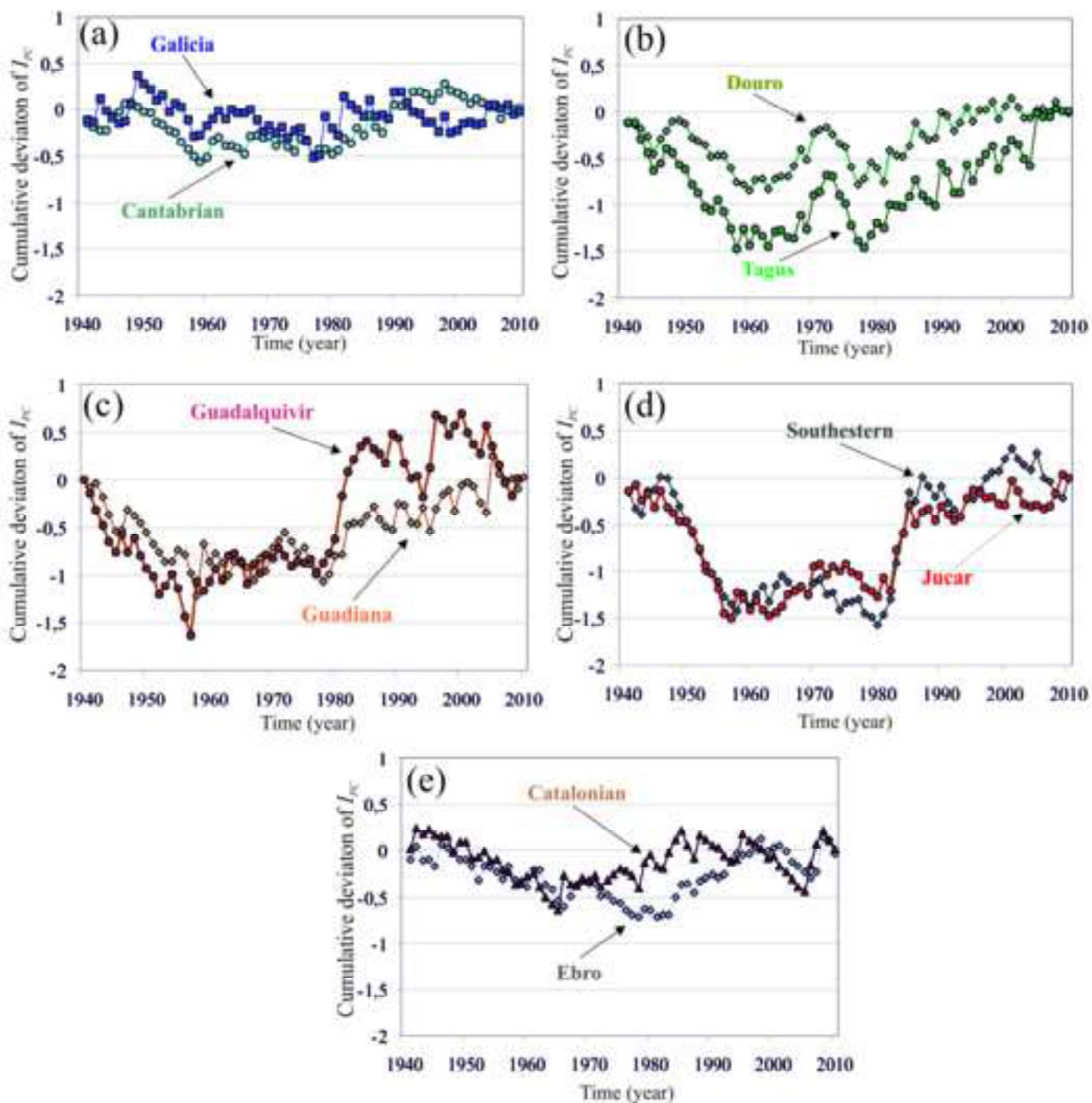


Table 1

I_{FM}	Average	Trend	V_N	I_D
Cantabrian	138.8	-0.06	0.14	0.19
Galicia	167.6	-0.15	0.24	0.36
Douro	72.8	+0.01	0.24	0.36
Tagus	83.7	-0.04	0.27	0.39
Guadiana	71.9	+0.01	0.29	0.41
Guadalquivir	120.7	-0.06	0.38	0.48
Southeastern	61.7	-0.04	0.26	0.35
Jucar	62.2	+0.07	0.20	0.26
Ebro	67.3	+0.01	0.16	0.23
Catalonian	82.2	+0.01	0.22	0.34

Table 3

<i>I_{PC}</i>	Average	% <i>I_{PC}</i> > 15	% <i>I_{PC}</i> < 10	Trend	<i>V_N</i>	<i>I_D</i>
Cantabrian	10.82	0.0	14.3	0.00	0.09	0.13
Galicia	12.30	7.1	0.0	0.00	0.13	0.20
Douro	11.83	4.3	7.1	0.01	0.12	0.18
Tagus	13.16	20.0	1.4	0.03	0.17	0.25
Guadiana	13.68	22.9	0.0	0.02	0.17	0.26
Guadalquivir	16.57	55.7	0.0	0.02	0.19	0.26
Southeastern	14.14	34.3	0.0	0.02	0.15	0.18
Jucar	12.16	7.1	4.3	0.02	0.14	0.20
Ebro	10.44	0.0	40.0	0.01	0.10	0.14
Catalonian	11.61	1.4	8.6	0.00	0.12	0.17

1 **Table 4**

<i>I_{PC}</i>	Cantabrian	Galicia	Douro	Tagus	Guadiana	Guadalquivir	South-eastern	Jucar	Ebro	Catalonian
Cantabrian	1.00									
Galicia	0.36	1.00								
Douro	0.46	0.64	1.00							
Tagus	0.27	0.45	0.80	1.00						
Guadiana	0.16	0.39	0.63	0.90	1.00					
Guadalquivir	0.14	0.34	0.44	0.67	0.81	1.00				
Southeastern	0.09	-0.03	0.23	0.39	0.43	0.57	1.00			
Jucar	-0.03	-0.18	0.16	0.25	0.11	0.13	0.59	1.00		
Ebro	0.36	0.06	0.40	0.27	0.17	-0.01	0.16	0.31	1.00	
Catalonian	-0.16	0.06	0.00	0.00	-0.03	-0.05	-0.02	0.22	0.34	1.00

2

Table 2

I_{FM}	Cantabrian	Galicia	Douro	Tagus	Guadiana	Guadalquivir	Southeastern	Jucar	Ebro
Galicia	0.28								
Douro	0.15	0.79							
Tagus	0.05	0.69	0.91						
Guadiana	0.06	0.59	0.80	0.93					
Guadalquivir	0.08	0.53	0.71	0.83	0.91				
Southeastern	0.04	0.16	0.36	0.48	0.62	0.66			
Jucar	0.00	0.07	0.26	0.30	0.36	0.35	0.61		
Ebro	0.36	0.38	0.53	0.45	0.43	0.39	0.22	0.38	
Catalonian	0.01	0.19	0.15	0.16	0.19	0.19	0.09	0.26	0.56

Figure captions

Fig. 1. Map of the division of the Spanish zones studied.

Fig. 2. Cumulative deviations of the Modified Fournier Index (I_{FM}) in the Spanish zones defined.

Fig. 3. Mobile variation coefficient using periods of eleven years of the Modified Fournier Index (I_{FM}) in the Spanish zones defined.

Fig. 4. Specific disparity of the Modified Fournier Index (I_{FM}) of rainfall in the Spanish zones defined.

Fig. 5. Cumulative deviations of the intra-annual concentration of rainfall (I_{PC}) in the Spanish zones defined.

Fig. 6. Specific disparity of the Precipitation Concentration Index (I_{PC}) of rainfall in the Spanish zones defined.

Fig. 7. Pairwise comparison between synchronous values of the indices I_{FM} and I_{PC} .

Fig. 8. Comparison of the estimated values of R factor and those of the aggressiveness risk R_A calculated (1991–2010) for the Guadalquivir river basin.